

## Inverse Solutions of the Prandtl-Meyer Function

O. Özcan,\* F. O. Edis,† A. R. Aslan,‡  
and İ. Pinar§

*Istanbul Technical University, Istanbul 80626, Turkey*

### Introduction

IN two-dimensional supersonic isentropic flow, an infinitesimal change in flow angle is equal to an infinitesimal change in the Prandtl-Meyer function.<sup>1,2</sup> Anderson<sup>1</sup> states that this function was first presented in the doctoral dissertation of Theodor Meyer who was a student of Ludwig Prandtl. The Prandtl-Meyer function  $\nu$ , which is an explicit function of the Mach number  $M$ , is defined by

$$\nu = \nu(M) = \alpha \tan^{-1}(\beta/\alpha) - \tan^{-1}\beta \quad (1)$$

where  $\beta$  is equal to  $\sqrt{M^2 - 1}$ , and the  $\alpha$  parameter is related to the ratio of specific heat coefficients  $\gamma$  by  $\alpha = \sqrt{(\gamma + 1)(\gamma - 1)}$ .

For a given turning angle of the flow, the value of the Prandtl-Meyer function becomes known and the Mach number is then calculated from Eq. (1). However, since Eq. (1) is an implicit relation for  $M$ , the calculation requires employment of either tables or approximate solutions. The iterative solution of Eq. (1) may appear to be a straightforward and adequate method for engineers who have powerful personal computers or workstations. However, for students and engineers who wish to solve a problem using a simple calculator, it is highly convenient to have an analytical expression that gives  $M$  in terms of  $\nu$  explicitly. Employment of such an inverse  $M(\nu)$  relation may also prove to be beneficial for the complex applications of the "method of characteristics." The characteristics method can be employed to solve not only two-dimensional, but also axisymmetric,<sup>1,2</sup> three-dimensional,<sup>1</sup> and nonisentropic<sup>2</sup> flows. The Prandtl-Meyer function appears in the so-called "compatibility equations," which are first-order ordinary differential equations satisfied along the Mach lines. Since Eq. (1) must be solved at a large number of grid points, computation time savings provided by an explicit  $M(\nu)$  relation may be substantially important.

The need for an inverse  $M(\nu)$  equation has become apparent to us in a recent application of the method of characteristics,<sup>3</sup> in which an exact inverse relation for a monoatomic gas ( $\gamma = 5/3$ ) was obtained. In this Note, the advantages of the exact inverse relation (in terms of computation time and accuracy) over the approximate methods employed to evaluate  $M$  are discussed. The exact inverse relation appears to be superior over the approximate methods considered in this Note. The success of the inverse relation has led us to an alternative approach for diatomic gases ( $\gamma = 7/5$ ): the least-square approximation was used to obtain fourth- and fifth-order polynomials as reasonably accurate inverse relations.

### Methods of Solution

Four different methods for obtaining inverse solutions of the Prandtl-Meyer function are considered. Method A is exact, whereas methods B, C, and D are approximate.

#### A. Exact Inverse Relation ( $\gamma = 5/3$ )

It appears that a general inverse solution of Eq. (1) does not exist. For the case of a monoatomic gas ( $\gamma = 5/3$ ),  $\alpha$  is equal to two, and Eq. (1) reduces to the following cubic equation:

$$\beta^3 - 3T\beta^2 - 4T = 0 \quad (2)$$

where  $T$  is equal to  $\tan(\nu)$ . The solution of Eq. (2) is the exact inverse relation given by

$$M = \sqrt{1 + (A + B + T)^2} \quad (3)$$

where  $A$  and  $B$  are given by

$$A = [2T(1 + \sqrt{1 + T^2}) + T^3]^{1/3}$$

$$B = [2T(1 - \sqrt{1 + T^2}) + T^3]^{1/3}$$

#### B. Approximate Inverse Relations

Approximate solutions of Eq. (1) can be found by using series expansions of the  $\tan^{-1}$  terms for large and small Mach numbers. The following equation is valid for a calorically perfect gas in hypersonic flow:

$$M = \frac{\alpha^2 - 1}{(\pi/2)(\alpha - 1) - \nu} \quad (4)$$

A slightly different form of Eq. (4) is presented in Ref. 2. The accuracy of Eq. (4), which is reasonably good for  $M > 5$ , increases with increasing Mach number.

For small Mach numbers around 1, the following approximate relation is valid for any value of  $\gamma$ :

$$M = \sqrt{1 + [\frac{2}{3}(\gamma + 1)\nu]^{2/3}} \quad (5)$$

Equation (5) is reasonably accurate only in a small range between  $1 < M < 1.1$  and, therefore, is not very useful for practical purposes.

The least-square approximation<sup>4</sup> was used to obtain accurate inverse relations for a diatomic gas. An attempt was made to obtain a single equation to represent the  $(M, \nu)$  variation in the range of  $0 < \nu < \nu_m$ , where  $\nu_m$  is the maximum value of the Prandtl-Meyer function ( $\nu_m$  is equal to 130.45 deg for  $\gamma = 7/5$ ). Since such a single and accurate equation could not be found, it was decided to obtain two separate polynomials valid in two different regions. These polynomials are given by

$$M = 1.03141 + 5.99196\eta - 15.6940\eta^2 + 58.3798\eta^3 - 87.6784\eta^4 + 58.6275\eta^5 \quad (6)$$

in the range of  $0 < \eta < 0.73$  ( $1 < M < 7$ ), and by

$$M = 1429.53 - 7420.13\eta + 14512.2\eta^2 - 12656\eta^3 + 4169.33\eta^4 \quad (7)$$

in the range of  $0.73 < \eta < 0.89$  ( $7 < M < 15$ ).

In Eqs. (6) and (7),  $\eta$  is the normalized Prandtl-Meyer function defined as  $(\nu/\nu_m)$ . An accurate polynomial inverse relation does not exist for very large Mach numbers. Equation (4), which may be used when  $M > 5$ , appears as one of the most accurate inverse relations for  $M > 15$ .

#### C. Approximate Solution by Iteration

Newton's method<sup>4</sup> can be used to solve Eq. (1) iteratively. Errors involved in the solution can be made very small by increasing the number of iterations. However, high accuracy is achieved at the expense of large computation times.

Received July 10, 1993; revision received Jan. 10, 1994; accepted for publication Feb. 1, 1994. Copyright © 1994 by the American Institute of Aeronautics and Astronautics, Inc. All rights reserved.

\*Professor, Faculty of Aeronautics and Astronautics.

†Research Assistant, Faculty of Aeronautics and Astronautics.

‡Associate Professor, Faculty of Aeronautics and Astronautics.

§Aeronautical Engineer.

#### D. Finite-Difference Approximation

The following equation is obtained by differentiating Eq. (1) and employing the first-order forward differencing:

$$\frac{\Delta M}{\Delta \nu} = \frac{M + [(\gamma - 1)/2]M^3}{\sqrt{M^2 - 1}} \quad (8)$$

where  $\Delta M$  and  $\Delta \nu$  are the changes in  $M$  and  $\nu$ , respectively. The right side of Eq. (8) is evaluated at known upstream values. Calculation error is determined primarily by the step size  $\Delta \nu$ . It must be noted that, in an application of the method of characteristics,  $\Delta \nu$  is affected by the solution and cannot be prescribed arbitrarily. Therefore, large step sizes (and significant errors) may arise in the solution of a flow (e.g., in expansion around a sharp corner).

Accuracy of the formulas presented in this section can be discussed in terms of the difference between the calculated Mach number and the exact  $M$  value given by Eq. (1). If this difference is called an error  $\delta M$ , the rms of the error  $\sigma$  is defined by

$$\sigma = \sqrt{(1/k) \sum (\delta M)^2} \quad (9)$$

where  $k$  is the number of data points in a particular Mach number range, and  $\Sigma$  is the summation operator. By definition,  $\sigma$  is zero for Eqs. (1) and (3).

#### Results and Discussion

Figure 1 shows the variation of the error in the Mach number  $\delta M$  with the exact Mach number for various inverse solutions of the Prandtl-Meyer function ( $\gamma = 7/5$ ). The rms error  $\sigma$  and the ranges over which  $\sigma$  is calculated are also given. Number of discrete data points [ $k$  in Eq. (9)] is equal to 5000 in calculating  $\sigma$  for the approximate inverse relations given by Eqs. (4), (6), and (7).  $k$  is equal to the number of integration steps  $N$  in calculating  $\sigma$  for Eq. (8).

The rms error  $\sigma$  for the finite difference solution is inversely proportional to the number of integration steps  $N$ . Values of  $\sigma N$  are roughly equal to 3.7 and 15.9 for the ranges of  $1 < M < 10$  and  $10 < M < 50$ , respectively. Integration of Eq. (8) is started from the middle of these ranges. By using the values given in Fig. 1 (for  $N = 50$ ), one can easily obtain that for  $N = 5000$ , values of  $\sigma$  are 0.0007 and 0.0032 for the ranges of  $1 < M < 10$  and  $10 < M < 50$ , respectively. Thus, when the step size  $\Delta \nu$  is sufficiently small, the finite difference solution is more accurate than the approximate inverse relations given by Eqs. (4), (6), and (7). The value of  $\sigma$  for the approximate inverse relations increases with increasing  $M$ .

The solution methods discussed in the previous section were employed in a specific application of the method of characteristics. Solution was obtained for the supersonic, isentropic flow in a diverging conical duct.<sup>3</sup> A schematic diagram of the axisymmetric flow geometry is shown in Fig. 2 together with the variation of the Mach number along the inner wall of the duct. The Mach number is uniform at the entrance, and  $\gamma$  is equal to 5/3. A 486-based personal computer was used in the computation.  $N = 60$  steps were taken in the radial direction  $R$ . Figure 2 presents the solutions obtained by using Eqs. (3), (4), and (8) in the range of  $5 < M < 50$ . The continuous line, which designates the solution produced by employment of Eq. (3), can be assumed to represent the exact solution. Flow-field results were independent of the grid size when  $N$  was in the range of  $40 < N < 60$ . The solution proceeded to  $X = 300$  in 350 streamwise steps.

Figure 2 shows that Eqs. (4) and (8) fail to perform as well as Eq. (3) for large  $X$  values ( $X > 100$ ). The finite difference approximation [Eq. (8)] gives quite accurate results for small values of  $X$ , where the step size  $\Delta \nu$  is sufficiently small. However, errors grow rapidly with increasing  $X$  as the step size

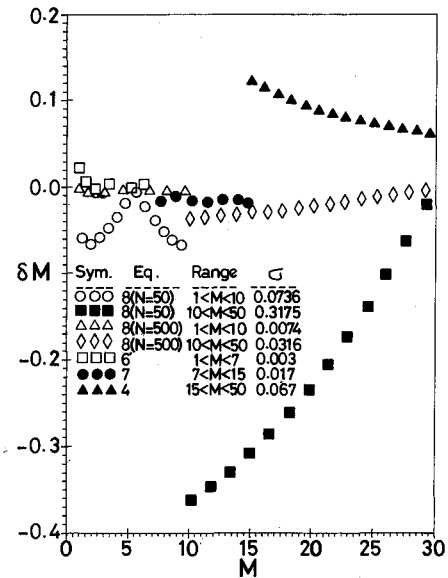


Fig. 1 Variation of the error in the Mach number  $\delta M$  with the exact Mach number for various equations ( $\gamma = 7/5$ ).

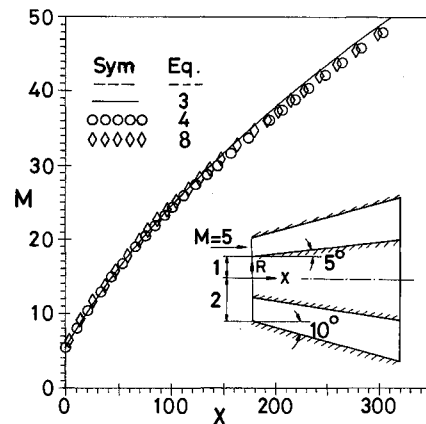


Fig. 2 Variation of the Mach number along the inner wall of a conical duct ( $\gamma = 5/3$ ) and a schematic description of the flow geometry.

$\Delta \nu$  becomes large. The accuracy of Eq. (4) is worse than that of Eq. (8) for small  $X$  values. However, accuracies of Eq. (4) and (8) are roughly equal for large  $X$  values. The rms error  $\sigma$  was calculated in the  $(M, X)$  plane by using the continuous line obtained by employing Eq. (3) as the exact solution. For the range of  $0 < X < 250$ , the rms error for Eq. (8) was roughly half of the rms error for Eq. (4). The problem of supersonic flow in a conical duct was also solved for the case of a diatomic gas. It was observed that when Eqs. (6), (7), and (4) were used in the ranges of  $5 < M < 7$ ,  $7 < M < 15$ , and  $15 < M < 50$ , respectively, the flow solution was more accurate than that obtained by using Eq. (8) for large  $X$  values ( $X > 100$ ).

Accuracy of the iterative solution (method C) can be made very good as stated earlier. When errors of  $\delta M = \pm 0.01$  and  $\delta M = \pm 0.001$  are tolerated during iteration, corresponding values of the rms error are equal to  $8.2 \times 10^{-4}$  and  $1.8 \times 10^{-8}$ . However, the computation time for the iterative solution is twice longer than that of Eq. (3). Computation times for the solutions of Eqs. (3), (4), (6), (7), and (8) are roughly equal.

#### Conclusions

The exact inverse relation presented in this Note appears to be superior to the iterative solution (in terms of computation time), and to the finite difference solution (in terms of

accuracy). A similar accuracy advantage of the approximate inverse relations over the finite difference solution may exist provided that the step size in a particular problem is sufficiently large. An obvious advantage of the inverse relations is the convenience of their employment compared to the use of tables of the Prandtl-Meyer function.

### References

- <sup>1</sup>Anderson, J. D., *Modern Compressible Flow*, McGraw-Hill, New York, 1984, pp. 108–119, 263–291.
- <sup>2</sup>Liepmann, H. W., and Roshko, A., *Elements of Gas Dynamics*, Wiley, New York, 1957, pp. 98, 99, 284–304.
- <sup>3</sup>Özcan, O., Aslan, A. R., Edis, F. O., and Pinar, İ., "Solution of Supersonic Flow by the Method of Characteristics," *Proceedings of the 8th Congress of National Mechanics* (Antalya, Turkey), ITU Matbaası, Istanbul, Turkey, 1993, pp. 489–498.
- <sup>4</sup>Gerald, C. F., *Applied Numerical Analysis*, Addison-Wesley, Reading, MA, 1980, pp. 15–20.

## Flow Study of Supersonic Wing-Nacelle Configuration

Kasim Biber\*

Wichita State University, Wichita, Kansas 67260  
and

Joel Mendoza†

NASA Ames Research Center,  
Moffett Field, California 94035

### Introduction

NACELLE/AIRFRAME integration is of major importance for aerodynamically efficient supersonic transport aircraft design and development.<sup>1–4</sup> For such aircraft, nacelles are commonly positioned beneath the wing to produce relatively low wave drag. In its proper location, the nacelle should normally have an attached normal shock at its inlet lip and capture the oncoming air mass without any spillage. When the nacelle is integrated with an aircraft wing, its flowfield is affected by the wing boundary layer, depending on the nacelle proximity to the wing surface. If the nacelle inlet is placed completely outside the boundary layer, then there will be an increase of wave drag. If the wing boundary layer flows through the nacelle, then loss in total pressure and distortion in the velocity distribution will result, causing a reduction in the engine performance.<sup>4</sup> Therefore, the boundary layer is usually removed by means of bleed and diverter before it enters the nacelle.<sup>3</sup> However, such a boundary-layer control requires detailed knowledge of both isolated and integrated wing-nacelle flowfields at various Reynolds numbers, angles of attack, and wing-nacelle gaps. This article presents the results of a flow visualization study, featuring supersonic wind-tunnel tests of wing-nacelle configurations. The tests were made at Reynolds numbers, based on nacelle length, about 25 times lower than its cruise flight counterpart. Also, the nacelle exit flow would be different in flight, due to the exhaust of an operating engine. This study brings some insight into the shock-boundary-layer flow interaction between the nacelle and wing and

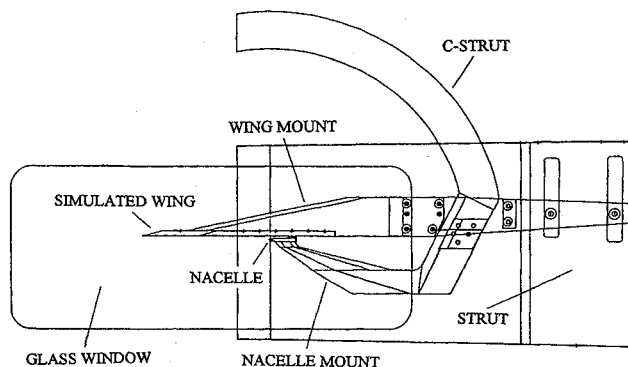


Fig. 1 Side view of the wing-nacelle model with the C-strut assembly in the tunnel test section.

examines the wing interference effects on the nacelle flow-field.

### Experimental Setup

The tests were conducted in a pressure-driven, intermittent, and open-circuit blowdown design supersonic wind tunnel with a 23- × 23-cm test section. The tunnel is equipped with a closed-loop servo mechanism that keeps the settling chamber pressure constant during tunnel runs.<sup>5</sup> The nacelle had a sharp-lip pitot intake with a 0.3-cm-diam, throughflow duct with a length-to-diameter ratio ( $L/D$ ) of 9.7 and a truncated-conical exterior with 2.5-deg semivertex angle. It was mounted to the tunnel C-strut assembly through its pylon (see Fig. 1). At its zero angle of attack  $\alpha$  setting, the nacelle was aligned with the test section centerline. The nacelle was positioned under a wing, 50D (diameter) streamwise distance from the wing apex. The wing simulated a delta wing, 2D thick, 75D long, and 25D wide flat plate planform with a 60-deg sweepback angle. When installed in the test section, the wing was parallel to the nacelle centerline, and supported separately from the nacelle so that there was no nacelle-wing strut to cause additional interference. The angles of attack were set to  $-2, 0, +2$ , and  $+4$  deg for each wing-nacelle gaps of 0.5D, 1D, 2D, and 3D, measured from the nacelle trailing-edge location.

Test conditions were characterized by the settling chamber pressure for the flow produced by Mach 2 nozzle blocks of the tunnel. Considering the losses downstream of the nozzle throat,<sup>6</sup> the actual test Mach number was  $1.94 \pm 0.02$ , as determined from a shock wave angle over the flat wing, and the ratio of test section pitot pressure to settling chamber pressure. Reynolds number was calculated from the settling chamber pressure and temperature for the prescribed Mach number. The viscosity was determined from Sutherland's formula as given in Ref. 7. Tests were made for Reynolds numbers, based on nacelle length, of  $1.16 \times 10^6$  and  $1.45 \times 10^6$ , respectively. Complete test cases are given in Ref. 8. The settling chamber pressure and, therefore, Reynolds number range, was limited by the nacelle/pylon strength. The flow unsteadiness in the settling chamber was observed qualitatively by the time history of stagnation pressures for about 10 s of tunnel runs.<sup>5</sup> There were fluctuations on the pressure signals, but these were below  $\pm 5\%$  for the present test values.

### Results and Discussion

Schlieren photographs were recorded for the flowfield of wing alone, nacelle alone, and then wing and nacelle together. Here the emphasis is given for the discussion of typical wing-nacelle results at the Reynolds number of  $1.45 \times 10^6$ . The nacelle had a conical oblique shock wave at its inlet lip, which remained steady and attached to the lip with  $\alpha$  changes. The flow inside the ducted nacelle was presumably fully turbulent and free of shock waves. This is mainly because the  $L/D$  ( $=9.7$ ) is not large enough for the internal boundary layer to create any choking flow conditions and subsequent supersonic

Received Feb. 22, 1994; revision received March 21, 1994; accepted for publication March 21, 1994. Copyright © 1994 by the American Institute of Aeronautics and Astronautics, Inc. All rights reserved.

\*Postdoctoral Research Associate, National Institute for Aviation Research, Box 93. Member AIAA.

†Aerospace Engineer, Advanced Aerodynamic Concept Branch, M/S 227-6.